

UNCLASSIFIED

Defense Technical Information Center  
Compilation Part Notice

ADP012211

TITLE: Temperature Dependence of Electroresistivity, Negative and Positive Magnetoresistivity of Graphite/Diamond Nanocomposites and Onion-Like Carbon

DISTRIBUTION: Approved for public release, distribution unlimited

This paper is part of the following report:

TITLE: Nanophase and Nanocomposite Materials IV held in Boston, Massachusetts on November 26-29, 2001

To order the complete compilation report, use: ADA401575

The component part is provided here to allow users access to individually authored sections of proceedings, annals, symposia, etc. However, the component should be considered within the context of the overall compilation report and not as a stand-alone technical report.

The following component part numbers comprise the compilation report:

ADP012174 thru ADP012259

UNCLASSIFIED

## Temperature Dependence of Electroresistivity, Negative and Positive Magnetoresistivity of Graphite/Diamond Nanocomposites and Onion-Like Carbon

Anatoliy I. Romanenko<sup>1</sup>, Olga B. Anikeeva<sup>1</sup>, Alexander V. Okotrub<sup>1</sup>, Vladimir L. Kuznetsov<sup>2</sup>, Yuriy V. Butenko<sup>2</sup>, Andrew L. Chuvilin<sup>2</sup>, C. Dong<sup>3</sup>, Y. Ni<sup>3</sup>

<sup>1</sup>Institute of Inorganic Chemistry SB RAS, Lavrentieva 3, Novosibirsk 630090, RUSSIA.

<sup>2</sup>Borisevsk Institute of Catalysis SB RAS, Lavrentieva 5, Novosibirsk 630090, RUSSIA.

<sup>3</sup>National Laboratory for Superconductivity, Institute of Physics Chinese Academy of Science, P.O.Box 603, Beijing 100080, China

### ABSTRACT

Here we present the result of measurements of electrical resistivity and magnetoresistivity of graphite/diamond nanocomposites (GDNC) and onion-like carbon (OLC) prepared by vacuum annealing of nanodiamond (ND) at various fixed temperatures. GDNC contain particles with a diamond core covered by closed curved graphitic shells. The electrical resistivity of annealed ND is characteristic of systems with localized electrons and can be described in terms of variable hopping-length hopping conductivity (VHLHC). The magnetoresistivity of OLC is negative in the range of field  $0 < B < 2$  T, and is positive at  $B > 2$  T. The conduction carrier concentration for OLC samples was estimated in the framework of the theory of negative magnetoresistance in semiconductors in the hopping conduction region. The free path length for conducting electrons at liquid helium temperature was estimated from the data on positive magnetoresistivity. The localization length of current carriers was also estimated. The determined parameters are in agreement with proposed structure model of OLC constructed using HRTEM data.

### INTRODUCTION

The study of electron transport properties of carbon materials is of interest due to wide practical applications and provides information on their structural perfection and electronic structure. The electronic properties of carbon materials vary over an enormous range due to the possibility of carbon to form different allotropes. Diamond is insulator, while graphite can be considered as a semi-metal. At the same time electronic transport and magnetic properties of graphitic materials strongly depend on their structure and the presence of defects. Thus the conduction carrier concentration ( $n$ ) depends on the defect number and structure [1], while the electrical and magnetic properties depend on this concentration [2, 3]. Influence of defects on the properties of multiwall carbon nanotube are considered in [4-7]. We have developed a method for production of graphite/diamond nanocomposites (GDNC) and onion-like carbon (OLC) based on controlled vacuum annealing of ND [8, 9]. In this work we study electrical resistivity and magnetoresistivity of GDNC and OLC prepared by ND annealing at various fixed temperatures.

## EXPERIMENTAL DETAILS

ND samples with an average particle size of 4.7 nm were prepared by an explosive method and isolated from the detonation soot by the oxidative removal of nondiamond carbon with a hot mixture of concentrated  $\text{H}_2\text{SO}_4$  and  $\text{HClO}_4$  acids in 1:1 proportion. Annealing procedure is described elsewhere [8, 10]. The diamond weight fractions in GDNC treated at different temperatures have been previously determined by the measurements of the true densities of the samples. Surface area of samples increases with annealing temperature from  $340 \text{ m}^2/\text{g}$  up to  $500 \text{ m}^2/\text{g}$ . Carbon black ( $286 \text{ m}^2/\text{g}$ ), graphitized soot (2700 K,  $9 \text{ m}^2/\text{g}$ ) and POCO graphite AF ( $12 \text{ m}^2/\text{g}$ ) were used as comparison carbon samples. Micrographs of the annealed products were obtained with a JEM-2010 transmission electron microscope.

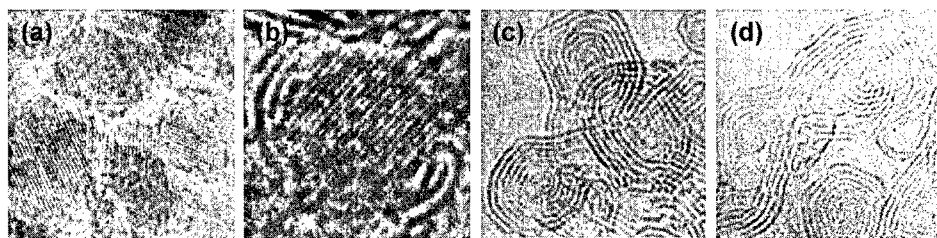
Four-probe  $d\epsilon$  measurements of resistivity vs. temperature  $\rho(T)$  at 4–300 K were performed. For details see in [10]. The samples were placed in glass tubes with a diameter  $d=2 \text{ mm}$  and length  $l=20 \text{ mm}$  to measure the electrical resistance. Silver wire was used to make contacts with the samples. We find that  $\rho(T)$  is highly reproducible for several measurements on different samples from the same batch.

The magnetoresistivity was measured in the field ( $B$ ) range 0 – 5.5 T at a temperature of 4.5 K using a model MPMS-5 SQUID magnetometer.

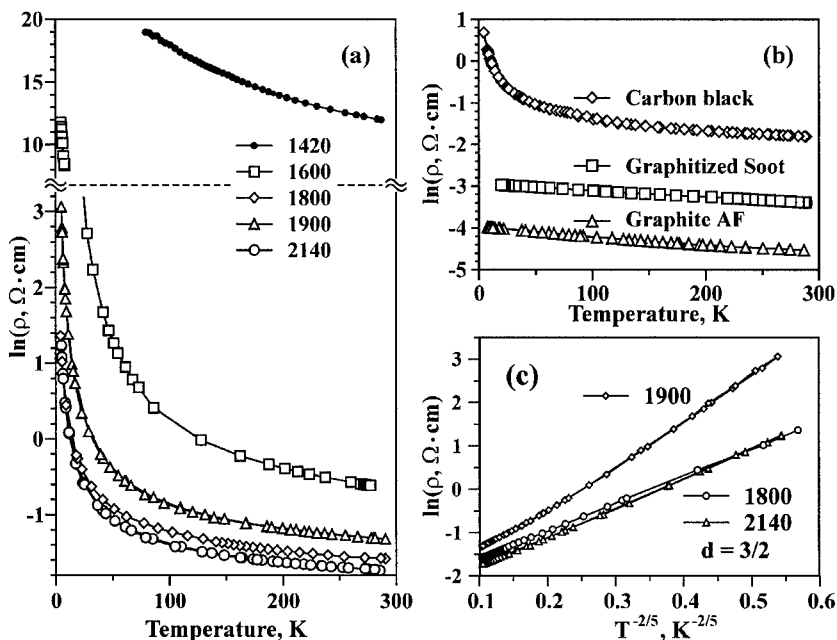
## RESULTS

Fig.1 presents typical TEM images of ND heated at four different temperatures. The dark straight contrast lines in micrographs (a) and (b) correspond to the (111) crystallographic diamond layers. The distance between these lines is  $2.06 \text{ \AA}$ . The dark curved lines in Figs.(b), (c) and (d) correspond to the (0002) crystallographic graphite layers ( $d \sim 3.4 \text{ \AA}$ ). The TEM images of the ND heated at 1170 K show no diamond to graphite transformation (Fig. 1a). ND graphitization started after ND annealing at 1420 K leading to the formation of 2-3 graphite layers on the surface of the diamond particles. The higher degree of graphitization is achieved with increase of annealing temperature (see Fig. 1b corresponding to ND annealing at 1600 K). The graphitization of diamond particles proceeds from the diamond surface toward the particle bulk. The diamond core can be clearly observed in some particles. Fig. 1 (c) presents the micrograph of the OLC produced at 1800 K. The ND particles are almost completely converted into the onion-like carbon. Fig. 1 (d) presents the micrograph of the OLC produced at 2140 K. Heating at this temperature results in the formation of hollow onion-like carbon particles. According to the true density measurements, diamond content ( $x$ ) in the samples heated at different temperatures varies with temperature:  $x_{1170} > 90\%$ ,  $x_{1420} = 0.86$ ,  $x_{1600} = 0.57$ ,  $x_{1800} = 0.15$ ,  $x_{1900} = 0.05$  and  $x_{2140} = 0.00$ .

The ND samples heated at temperatures lower than 1170 K, which do not exhibit any surface graphitic species, have the highest resistivity values (higher  $10^9 \Omega \text{ cm}$ ). As diamond graphitization occurs the resistivity of the corresponded samples drop significantly. The temperature dependencies of resistivity of ND annealing products and carbon comparison standards are presented in Fig.2. For ND annealing products treated at temperatures higher than 1600 K the values of resistivity at 300 K lie in the range  $0.2\text{--}0.5 \Omega\text{-cm}$  and are comparable to



**Figure 1.** HRTEM micrographs of ND samples annealed under vacuum at (a) 1170, (b) 1600, (c) 1800, (d) 2140 K.



**Figure 2.** Temperature dependence of resistivity of (a) ND annealing products and (b) comparison carbon samples. (c) – example of data fitting in the plot of  $\ln(\rho)$  versus  $(1/T)^\alpha$ , here  $\alpha=2/5$  [10]. See text for a definition of  $d$ .

that of carbon black (Fig.2 b). It should be mentioned that despite the tendency to a decrease of resistivity with increasing annealing temperature the resistivity of the sample treated at 1900 K is higher than the resistivity of the samples treated at 1800 and 2140 K in the whole temperature region.

For all samples annealed at temperatures higher than 1170 K the electrical resistivity shows the temperature dependence typical of systems with VHLHC [11]. This dependence takes place

in strong disordering materials with a length of local disordering of about a few interatomic distances [12-14]. For these systems, the temperature dependence of resistance  $\rho(T)$  may be described by the equation:

$$\rho(T) = \rho_0 \exp(T_0/T)^\alpha \quad (1)$$

where  $\rho_0$  and  $T_0$  are constants. Fig. 2c shows the resistivity data of ND annealed products plotted in coordinates of  $\ln \rho$  vs  $(1/T)^\alpha$  where  $\alpha$  is varied from 2/5 to 2/3. One can clearly see that the data of ND annealed at 1800 K, 2140 K plotted so approximate straight lines with  $\alpha$  equal to 2/5. Data of OLC produced at 1900 K approximate straight lines with  $\alpha$  equal to 1/2. The value of  $\alpha$  correlates with dimensionality  $d$  of the movement space for current carriers as  $\alpha = 1/(1+d)$ . For CDNC prepared at 1420 and 1600 K the following values for  $d$  were estimated: 1 and 0.5 respectively. For OLC (prepared at 1800, 1900 and 2140 K) dimensionality varies as 1.5, 1 and 1.5. It should be noted that for carbon black (within the interval 4–300 K) and graphitized soot (4–40 K) the resistivity data in graph of  $\ln \rho$  vs  $(1/T)^\alpha$  approximate a straight lines with  $\alpha = -1/4$  that corresponds to a dimensionality  $d$  equal to 3.

The value of  $d = 1$  corresponds to the case when current carriers move along the one-dimensional chains of carbon atoms. A value of  $d = 0.5$  corresponds to the case of formation of one-dimensional chains with length of chains being less then the hopping length in VHLHC.  $d \geq 1.5$  corresponds to the formation of two dimensional conductive planes. For details see [10].

The dependencies of resistivity of OLC on the applied magnetic field measured at 4.2 K are presented in Fig.3. The magnetoresistivity of OLC is negative in the range of field  $0 < B < 2$  T, and is positive at  $B > 2$  T. The free path length  $l$  for conducting electrons at liquid helium temperature was estimated from the data on positive magnetoresistivity [15]. Fig.3a presents data plotted in coordinates of  $\rho(B)/\rho(0)$  vs  $B^2$ . The solid lines are fits by equation (2) with parameters:  $l \sim 12$  Å for OLC (1800 K);  $l \sim 18$  Å for OLC (2140 K).

$$\rho(B)/\rho(0) \equiv B^2/(lr_L)^2 \quad (2)$$

The conduction carrier concentration  $n$  for OLC samples was estimated in the framework of the theory of negative magnetoresistance in semiconductors in the hopping conduction region (with the proposition  $n \sim n_c$ , where  $n_c$  is the critical concentration). Fig.3b presents data plotted in coordinates of  $\ln[\rho(B)/\rho(0)]$  vs  $B$  [16]. The solid lines are fits to equation (3) with parameters:  $n \sim 8 \cdot 10^{21} \text{ cm}^{-3}$  for OLC prepared at 1800 K and  $n \sim 3 \cdot 10^{21} \text{ cm}^{-3}$  for OLC prepared at 2140 K.

$$\ln[\rho(T, B)/\rho(T, 0)] = -A\{(eB/hc)n^{-2/3}\} \ln[\rho(T)/\rho_0] \quad (3)$$

Here  $A$  is a number of the order unity. As we found the electrical conductivity of GDNC and OLC is characteristic for the systems with localized electrons and can be described within the model of VHLHC. These systems can be characterized with the value of localization length  $\xi$  of current carriers, which determines the tunneling probability of conducting electrons. The  $\xi$  value depends not only on the barrier height but also on the proximity to the metal-insulator transition point and can be described with equation (4) [16].

$$\xi \sim a(n_c - n)^{-1/2} \quad (4),$$

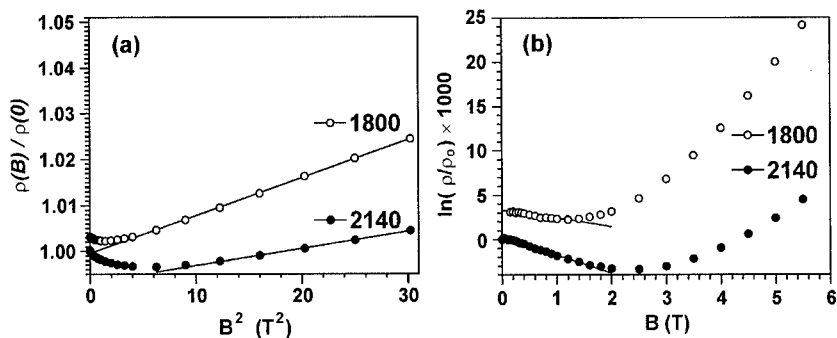


**Figure 3.** The dependencies of specific resistivity of OLC on magnetic field at 4.2 K: a)  $\rho(B)/\rho(0)$  vs  $B^2$ ; b)  $\ln[\rho(B)/\rho(0)]$  vs  $B$ .

where  $n_c$  is the critical concentration and  $n$  is concentration of carriers ( $a \sim 1$ ). We have used equation (4) for a crude estimate of the minimal value of localization length  $\xi$  (when  $n \ll n_c$ ). In our case it was equal to 60-100 nm. This value is comparable with the size of OLC aggregates (0.1- 0.5  $\mu\text{m}$ ).

## CONCLUSIONS

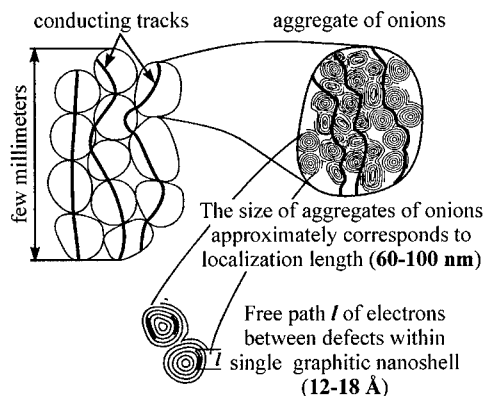


**Figure 4.** The scheme of three scales of OLC particle organization. The hard solid lines correspond to current conduction tracks.

Fig. 4 summarizes the data on the conductivity of OLC. The carbon powders obtained by annealing of ND consist of the OLC aggregates. Within the aggregates onions are linked to each other with defect graphite-like sheets and C-C bonds. Some part of the onions is presented by elongated particles with linked external graphitic layers and closed quasi-spherical shells. Study of X-ray emission spectra of OLC combined with quantum-chemical simulation for the characterization of their electronic structure led us to the conclusion that the onions produced by ND annealing at the intermediate temperature (1400-1900 K) have holed structure of internal shells [17]. The origin of such defects accompanying the OLC formation can be explained in terms of deficit of diamond carbon atoms in the diamond/graphite interface to form perfect fullerene-like shells during ND annealing [17].

The free path length of electrons within OLC particles is comparable with the size of graphitic fragments within holed structure of single onion ( $l \sim 12 \pm 2$  Å). When their holed structure is annealed with the formation of hollow polygonized structures the free path length of the electron increases up to  $18 \pm 2$  Å. The size localization length of current carriers is comparable with the size aggregates of OLC particles.

## ACKNOWLEDGMENTS

The work was supported by the Russian Foundation of Basic Research (Grant No. 00-02-17987), INTAS (Project Nos. 97-1700, 01-237) and CRDF grant REC 008.

## REFERENCES

1. A. S. Kotosonov, JETP Lett. **43**, 1, 30 (1986).
2. A. S. Kotosonov, JETP **93**, 5(11), 1870 (1987).
3. A. S. Kotosonov, Solid State Phys. (Rus.) **33**, 2616 (1991).
4. A. S. Kotosonov, and S. V. Kuvshinnikov, Phys.Lett. **A230**, 377 (1997).
5. A. S. Kotosonov, and D. V. Shilo, Carbon, **36**, 1649 (1998).
6. A. S. Kotosonov, JETP Lett. **70**, 468 (1999).
7. A. S. Kotosonov, and V.V. Atrazhev, JETP Lett. **72**, 2, 76 (2000).
8. V.L.Kuznetsov, A.L. Chuvilin, Yu.V.Butenko, I.Yu. Mal'kov, V.M. Titov, *Chem. Phys. Lett.*, **222**, 343 (1994).
9. Yu.V. Butenko, V.L.Kuznetsov, A.L. Chuvilin, V.N. Kolomiichuk, S. V. Stankus, R. A. Khairulin, B. Segall, J. Appl. Phys., **88**, 4380 (2000).
10. V.L.Kuznetsov, Yu.V.Butenko, A.L. Chuvilin, A.I.Romanenko and A.V.Okotrub, *Chem. Phys. Lett.*, **336**, 397 (2001).
11. N.F. Mott, E.A. Davis, *Electron processes in non-crystalline materials*, Clarendon Press, Oxford, 1979.
12. A.I. Romanenko, Solid State Phys. (Russian). **27**, 2526 (1985).
13. A.I.Romanenko, in: A.A. Aronov, A.I. Larkin, V.S. Lutovinov (Eds.), *Progress in high temperature superconductors*, World Scientific, Singapore. **32**, 72 (1992).
14. A.I. Romanenko, N.F. Zakharchuk, N.G. Naumov, V.E. Fedorov, U-Hyon Paek, *Materials Research Bulletin*, **32**, 1037 (1997).
15. A. A. Abrikosov, *Bases of metal theory (Rus.)*, Nauka, Moscow (1987).
16. B. L. Altshuler, A. G. Aronov, and D. E. Khmel'nitskii, JETP Lett. **36**, 5, 157 (1982).
17. A.V. Okotrub, L.G. Bulusheva, V.L. Kuznetsov, Yu.V. Butenko, A.L. Chuvilin, and M.I. Heggic, *J. Phys. Chem.* **A105**, 9781 (2001).